Comparison Between IGS and Three ITRS Realizations

Jiao Liu
SHAO: Shanghai Astronomical Observatory Chinese Academy of Sciences https://orcid.org/0000-0002-7298-557X

Junping Chen (junping@shao.ac.cn)
Shanghai Astronomical Observatory Chinese Academy of Sciences

Peizhao Liu
Shanghai Astronomical Observatory Chinese Academy of Sciences

Weijie Tan
Shanghai Astronomical Observatory Chinese Academy of Sciences

Danan Dong
East China Normal University

Weijing Qu
Shanghai Astronomical Observatory Chinese Academy of Sciences

Full paper

Keywords: IG2, realizations of ITRS, Helmert transformation

Posted Date: September 23rd, 2020

DOI: https://doi.org/10.21203/rs.3.rs-78689/v1

Abstract

Four space geodetic techniques (IGS, SLR, VLBI and DORIS) contribute to the realizations of International Terrestrial Reference System (ITRS). The GNSS-derived terrestrial reference frame generated from the second reprocessing campaign (repro2), named IG2, act as the IGS input to the most recently three realizations (ITRF2014, DTRF2014 and JTRF2014). Its origin and orientation are aligned to the IGb08, and its scale is defined by using the igs08.atx satellite antenna phase center offset (PCO) values. To study the consistencies and discrepancies between IGS solutions and the three ITRS realizations, we corrected the IG2 solutions to be uniform with the IGS14 frame and perform Helmert transformation to compare the IGS frame and the three ITRS realizations. Results indicate that IGS frame is more stable than the two secular frames especially in the periods after 2015. The similarity transformation parameters between the corrected IGS solutions and ITRF2014 show excellent agreement with a notable mean z-offset of around 1 mm. The transformation parameters between the corrected IGS solutions and DTRF2014 show linear discrepancies in the three categories parameters, where the origin offsets are around less than 5.5 mm, rotational alignment is consistent at the level of 4.5 uas/yr (about 0.15 mm/yr) and the scale exhibits a stable offset of 0.16 ppb. Unlike the two secular frames, distinct seasonal signals and interannual variations of translation time series can be observed from the comparison between JTRF2014 and the IGS solutions. The orientation of JTRF2014 is in worst agreement with the IGS solutions, which is related to biased no-net-rotation (NNR) condition due to weekly center of network (CN) variations. Moreover, the scale defined by JTRF2014 suffer from large instability variations over time.

Introduction

The realization and maintenance of a Terrestrial Reference Frame (TRF) is foundational for understanding and investigation of the linear and nonlinear time variations of the solid earth's shape caused by various geophysical processes, like plate tectonics (Argus and Heflin 1995; Altamimi et al. 2012; Argus et al. 2014), glacial isostatic adjustment (Argus 1996; Argus et al. 1999) and large scale surface mass (atmosphere, snow, glacier, soil moisture and ground water storage) variations (Borsa et al. 2014; Fu et al. 2015), and sea level rise (Gross et al. 2009; Blewitt et al. 2010; Collilieux and Woppelmann 2011; Woppelmann and Marcos 2016). The TRF also plays critical role as the reference in operational geodesy applications, such as precise point positioning, precise orbit determination, and natural hazard monitoring. High accuracy, consistency and long-term stability of a TRF are required for geophysical and geodetic applications, demanding that the accuracy and stability of the TRF to be at 1 mm and 0.1 mm yr-1 level (Altamimi et al. 2008; Gross et al. 2009).

The most recent realizations with the combination strategy and the physical model enhancement are ITRF2014 (Altamimi et al. 2016), DTRF2014 (Seitz et al. 2016), and JTRF2014 (Angermann et al. 2017) respectively. All the three realizations are computed on the basis of the data from four space geodetic techniques (Angermann et al. 2020), including Global Navigation Satellite System (GNSS), Doppler Orbitography and Radiopositioning integrated by Satellite (DORIS), Satellite Lasor Ranging (SLR), and Very Long Baseline Interferometry (VLBI). As no single space geodetic technique is able to provide the full

reference frame-defining parameters, the strengths of the four contributing space geodetic techniques are integrated and their weaknesses and systematic errors are mitigated. Although the identical input data was used, the three realized TRFs are defined in different conception (Angermann et al. 2020). While ITRF2014 and DTRF2014 are based on a piecewise linear motion model of global distributed stations with positions at a reference epoch and velocities, the JTRF2014 is a time series-based frame. The two secular solutions, ITRF2014 and DTRF2014, are established following a two-step procedure: (1) stacking the individual time series to estimate a long-term solution for each space technique; (2) combining the four long-term solutions together by means of local ties at co-location sites. However, ITRF2014 and DTRF2014 are computed by the combination of solutions and normal equations respectively (Seitz et al. 2012; Seitz et al. 2016). Another two differences about non-linear station motions are that: the sites affected by major earthquakes are described by post-seismic deformation (PSD) models in the ITRF2014, while the DTRF2014 simply uses piece-wise linear models to represent the earthquake-affected station positions; atmospheric and hydrological non-tidal loading (NTL) was applied within the DTRF2014 computation, while seasonal (annual and semiannual) signals of station positions were estimated within the ITRF2014 computation. What's more, the averaging strategies for scale are the arithmetic mean and the weighted average of VLBI and SLR for the ITRF2014 and the DTRF2014 respectively. Different combination strategies and analysis strategies used by the realized TRFs may lead to differences of reference frame defining parameters. Linear differences may be presented between the two secular frames, and non-linear variations will certainly appear in JTRF2014.

However, the non-negligible fact is that the deficiency comes from imperfect models and inhomogeneous distribution of stations used by individually geodetic techniques and combination model for local tie techniques at co-location sites, which results in quality and alias signals, so that presenting great challenges to acquire a terrestrial frame when describe the actual shape of the solid earth. Firstly, the secular frames realized of ITRF2014 and DTRF2014 neglect the non-linear variation of origin and their access to the period beyond the life-span of the TRF are based on simple extrapolation, which is inaccurate. Secondly, the origin and scale between the two consecutive ITRFs contain distinct linear discrepancies because of analysis advancement and quality and quantity improvement of data. Thirdly, scale determined by SLR and VLBI affected by technique-dependent errors maybe not credible even they are averaged carefully. Particularly, epoch-averaged scale from SLR and VLBI is heavily blocked by the degradation of the SLR ground network over time. Finally, the orientation of quasi-instantaneous are biased by continuous variation of CN.

International GNSS Service (IGS) plays a crucial role in the realization and densification of TRFs due to the largest number and the extensive distribution of geodetic stations in the ground and artificial satellites in the space among the four geodetic techniques, along with orders of magnitude improvement in data precision. On one hand, orientation definition of a TRF generally relies on a well-distributed GNSS network, which other space techniques are inaccessible because of limited ground sites and distributions. On the other hand, GNSS sites act as a connector at co-location sites when combining the four contributing techniques, which benefit from precise position and lower-cost construction of sites. Besides the essential status in the realization of ITRS, the IGS realizations of the ITRFs, such as IGb08 and IGS14,

were constructed as the reference datum for precise orbit determination and deformation monitoring etc. As the real-time updating of the IGS datum, non-linear variations, including real geophysical crustal motions, artificial variations, and unexplained variations (Ray 2008, Altamimi et al. 2019) are contained in the time series of station positions, which is superior to the secular frames with only linear information included. In addition, during the period between the up-to-date realizations of ITRS and next release generate, IGS solutions can provide ultimate accurate position of ground sites based on minimal constraint applied to a subset of core stations.

The IG2 solutions is based on the second IGS reprocessing campaign (repro2) to provide homogeneous IGS inputs to the three mentioned TRF realizations (Rebischung et al. 2016; Bloßfeld et al. 2018). GNSS data span from 1994 to 2014 were reanalyzed by nine different Analysis Centers (ACs) using the latest available models and methodology. Since GNSS technique is insensitive to Center of Mass (CM), the origin of the final combined solution aligned to IGb08 with minimum constraints (no-net-translation, NNT) applied to a subset of core stations (Petit and Luzum 2011). The orientation aligned to IGb08 with NNR applied to the same core network. The scale is defined by using the igs08.atx containing satellite PCO values (Rebischung et al. 2016; Ray 2013b; Ray 2013). The IGS solutions are based on IGb08 frame till Feb. 28, 2017, then they are generated based on IGS14 frame.

Due to the model deficiency, ITRF2014, DTRF2014 and JTRF2014 unavoidably exhibit accuracy degradation. In this paper, we use the continuously observed GNSS frame solutions, i.e. the IG2 solutions from Jan. 1995 to Jan. 2015 and the IGS solutions from Feb. 2015 to Jul. 2020 as reference bench mark, to study the signals in the three realizations and their performance in frame prediction, so as to give valuable information for their future realizations. Helmert transformation approach and related parameters are used to study the discrepancies and consistencies between the IGS solutions and up-to-date realizations. In Sect. 2, IGS station network and selected station network used to perform similarity transformation are illustrated. Then, the IGS solution are compared to ITRF2014, DTRF2014 and JTRF2014 and their predictions in the following sections.

Selected Gnss Station Network

As an indispensable component of TRS realizations, IG2 reveals its predominant status in time series combination of global frame especially due to the extensive distribution of ground stations and the accurate determination of station positions. The stations contributing to the IG2 and the ITRF2014 are displayed in Fig. 1. As seen in Fig. 1, the distribution of the involved stations is globally but relative sparse in southern hemisphere and ocean areas (Wu et al. 2017), which brings obstacle in precise assessment of geo-center motions (Rebischung et al. 2014, 2016; Rietbroek et al. 2012, 2014; Wu et al. 2015, 2017). Station number evolution of individual ACs illustrated in Fig. 2 demonstrates that most ACs' station number, except GTZ and ULR, tend to become stable after 2004, which indicate the maturity of the GNSS network. In addition, each daily AC solution consists of unique network geometry and uses inconsistent processing strategies, so unequal amplitude and phase of seasonal signals, even spurious signals, may

be contained in position time series of the ACs. All the available signals are combined and spurious signal are mitigated in the IG2 time series through the advantageous combination strategies used by IGS.

Helmert transformation is a typical method for reference frame analysis and its parameter estimates may be affected by the network distribution. A stable and well distributed network is selected with 165 ground stations, which is displayed in Fig. 3, and its number evolution is displayed in Fig. 4. The selection criteria contain two points: continuity and stability of the stations participating in the daily solutions. All the stations with data length longer than 2 years over a consecutive periodic of time, among them 12 suffer from the effect of major earthquakes. We believed that the selected station network is credible when acquiring Helmert transformation results.

Comparison between ITRF2014 and IGS

The ITRF2014 is a superior release compared to past ITRS realizations with two innovations implemented in construction of the ITRF2014: First, the PSD models along with linear station motions are provided for the stations affected by major earthquakes; Second, seasonal signals (annual and semi-annual) are estimated at stacking step for the purpose of acquiring more precise velocities of ground stations. As it precisely modeling the actual trajectories of station position time series, ITRF2014 is demonstrated to be a more robust secular frame.

In this section, IG2 daily solutions from Jan. 1995 to Jan. 2015 and IGS solutions from Feb. 2015 to Jul. 2020 are selected to compare with the ITRF2014 positions of selected stations, where the station coordinates of the ITRF2014 after Jan. 2015 are from the prediction based on ITRF models.

In the following of this paper, both the IG2 and IGS are uniformly called IGS. The IGS and ITRF2014 station coordinate time series for ALBH and MIZU were plotted in Fig. 5. In Fig. 5, one can clearly see constant offsets between ITRF2014 and IGS of the two sites. Such a non-negligible offset may reflect the inconsistent reference origin of the two frames. In addition, the site ALBH suffer from an abrupt break because of antenna change in Sep.15 2015, while ITRF2014 model miss the corresponding corrections. The site MIZU suffers from an increasing position errors in the ITRF2014 models due to inaccurate position prediction after Jan. 2015. Such phenomena indicate that using ITRF2014 coordinates at a reference epoch and velocities to extrapolate positions of ground sites are inappropriate to a certain extent. In addition, although non-linear signals are contained in the IGS time series, IGS is actually a linear frame whose origin and orientation are aligned to the IGb08/IGS14.

In order to further access the discrepancies between the two linear frame, Helmert transformation is performed between them. In the Helmert transformation processing, the outlier rejection thresholds are 10, 10, 30 mm in N, E, U components, respectively (Fritsche et al. 2014). Figure 6 displays translation, rotation, and scale time series estimated between the ITRF2014 and IGS solutions. The discontinuity occurs in Feb. 2017 attribute to the fact that IGS daily solutions are based on IGS realizations of ITRF2014 (i.e. IGS14) after Feb. 28, 2017. The averages of translation time series are statistically approach to zero after that time, while greater offsets are present in scale offsets, which is related to the

differential scale rate between the ITRF2014 and IGS solutions (Rebischung et al. 2016b). Rotation parameters in all components with negligible offsets and temporal variations along the full time-span demonstrates excellent agreement of orientation between IGS and ITRF2014 attributing to NNR constraint applied to continuous ITRFs.

Non-zero constant offsets of X, Y components and an apparent drift from Z component translation time series before Feb. 28, 2017 represent the discrepancy between the secular ITRF2014 origin and the long-term mean origin of IG2. The slope 0.12 mm/yr and − 0.03 ppb/yr are found in Z component of translation and scale time series, which is coincident to transformation parameters from ITRF2014 to ITRF2008. Actually, the origin and orientation of IGS are aligned to the IGb08 before Feb. 28, 2017, and the scale of IGS is determined by using the igs08.atx (Rebischung et al. 2016). Both the drift of Z component translation time series and scale offsets suggest precision improvements coming from contributing reprocessed data because of corresponding improved technique-specific analysis strategies in ITRF2014. Greater biases in the period from 1995 to 1998 are caused by a poor geometry distribution of usable GNSS stations selected for the minimum condition in IGS daily solutions.

In order to obtain homogeneous result of Helmert transformation comparison, the IGS solutions before Feb. 29, 2017 are corrected to be of uniform datum with the IGS14 using the transformation parameters estimated between IGS14 and IGb08. After the frame transformation, the transformation parameters and their amplitude spectrum are displayed in Fig. 7. The time series of seven transformation parameters become more consistent after the correction especially for translation parameters. However, an offset of less than 1 mm before 2015, although less than its magnitude in Fig. 6, can be observed in Z component of the translation time series, which could be interpreted by the antenna calibration updates differences of the specific stations between igs08.atx and igs14.atx (Rebischung et al. 2012) and misalignment to the secular frame (i.e. IGb08) when generating the IGS solutions. The remaining discrepancies appear in the translation time series from Oct. 2012 to Jan. 2017 may be caused by the geometry degradation of IGb08, and prediction mis-modeling of ITRF2014 after Jan. 2017. Scale offsets after Jan. 2017 with an offset about − 0.25 ppb is coincident with the long-term scale rate difference of 0.026 ppb/yr and zero-offset at epoch 2010.0 between ITRF2014 and IGS14-based IGS solutions (Rebischung et al. 2016b). Thus, scale of IGS14-based solutions defined by igs14.atx is not exactly equal to scale of ITRF2014 over time.

The non-linear signals result from IGS time series related to real geophysical signals and spurious signals induced by orbit modeling deficiencies et al. Among all seasonal and dracontic signals, the biggest amplitudes at annual signals are less than 0.25 mm for translation offsets and less than 7 uas for rotation offsets, which could benefit from the advantageous combination strategies used by IGS. While non-linear scale offsets with annual amplitude about 0.25 ppb in last panel of Fig. 7 are mostly expected from the non-linear vertical deformations of the selected station network (Altamimi et al. 2011, Collilieux et al. 2010) and just a fraction from imperfection in the adopted satellite antenna z-PCO values (Ge et al. 2005).

Comparison between DTRF2014 and IGS

The DTRF2014 is another secular reference frame with normal equations of the contributing space techniques are combined rather than solutions are combined in the ITRF2014 construction (Seitz et al. 2016; Angermann et al. 2020). What's more, piece-wise linear models and atmospheric and hydrological NTL was applied for DTRF2014 to describe station non-linear motions (Seitz et al. 2016). Correspondingly, piece-wise linear models used for stations affected by major earthquakes may cause a certain departure from the real trajectory after major earthquakes. As an instance, the coordinates time series of station ASPA are displayed in Fig. 8. In Fig. 8, we find that using the ITRF2014 models to fit IGS time series perform better than the DTRF2014 especially after 2015.0. As post-seismic response may last several years, the affected stations will contain irregular error signals which is different from systematic errors. And applying NTL models to correct individual daily or weekly solutions motions will generate position and velocity differences. Again, there are constant offsets existing in most station position time series between DTRF2014 and IGS, but the magnitude may differ from the previous section in the comparison between ITRF2014 and IGS, which indicate inconsistent reference origin and velocities of ground sites between ITRF2014 and DTRF2014.

We perform Helmert transformation between the DTRF2014 and the corrected IGS time series, and employ identical outlier rejection condition as utilized between ITRF2014 and IGS. The corrected transformation parameter time series and their amplitude spectrums are displayed in Fig. 9. The offset and drift results from linear regressions to the transformation parameter time series are provided in Table 1 at epoch 2010.0.

Table 1
Offsets at epoch 2010.0 and drifts of the transformation parameter time series estimated between DTRF2014 and IGS

	T_X	T_Y	T_Z	R_X	R_Y	R_Z	Scale
offset	0.8	1.3	-1.9	-2.0	-12.7	-2.5	0.16
drift	0.03	0.12	-0.19	-2.3	-4.0	4.5	-0.001

Note: Unit for translation parameters are mm, for rotation parameters are uas, for scale parameter is ppb; Unit for translation parameters are mm/yr, for rotation parameters are uas/yr, for scale parameter is ppb/yr.

The translation offsets are at mm level. And their drifts are statistically not equal to zero, which indicates non-negligible linear discrepancies between IGS and DTRF2014. The RMS in the fitting of translation time series suggest that the origin agreement between the two frames is at the level better than 5.5 mm. As reveled in the previous section, the IGS frame is basically the same as ITRF2014, and both ITRF and DTRF defines their origin using identical data observed by SLR. we conclude that inconsistent analysis strategies, especially non-linear signals assessment methods at stacking step, used by the ITRF and DTRF contributed to linear discrepancies of origins in all components.

Time series of rotations between DTRF2014 and IGS exhibit evident linear signals in all three components. Maintenance of orientation relies on NNR constraint applied to a well distributed GNSS network and a set of well-behaved stations. Unlike the ITRF2014, whose orientations are aligned to ITRF2008, the orientation of DTRF2014 is aligned to DTRF2008 (Seitz 2020). The linear inconsistence between DTRF2014 and ITRF2014 may result from the biased NNR condition applied on two distinct GNSS station networks at different reference epoch by the two frames (Bloßfeld et al. 2014). In addition, partly because of correlation between translation and rotation parameters, the linear discrepancies of translation were observed in rotation offsets between the two frames. The agreement between the two frames become worse after 2014, which may be related to faster decay of DTRF2014 linear modeling.

An offset 0.16 ppb and statistically zero drift is found in scale offsets before Feb. 2017, which indicates scale differences determined by ITRF2014 and DTRF2014. Linear behaviors of scale differences are the consequence of scale processing strategies adopted in averaging the VLBI/SLR information and local ties (Moreaux et al. 2020). Scale offsets after Feb. 2017 are close to zero, so the scale define by igs14.atx of IGS solutions seems closer to scale of DTRF2014 during this period. However, both annual and semiannual amplitude of 0.25 ppb and 0.05 ppb, respectively, are quite equivalent with scale offsets estimated between ITRF2014 and IGS time series. Therefore, non-linear variations of the selected station network presented in scale offsets are much similar, which is not influenced by scale processing strategies of discrepancies between ITRF2014 and DTRF2014.

Except the non-linear signals in scale offsets, the biggest spectral peak less than 0.3 mm is visible in Y component of translation time series, and distinct peaks can also be observed at several harmonics of the GPS draconitic year. All the amplitudes of spectral peaks are slightly unequal to amplitude spectra estimated between ITRF2014 and IGS, which indicate coordinate differences induced by different combination strategy, non-linear signals and PSD models.

Comparison between JTRF2014 and IGS

Unlike the secular frames ITRF2014 and DTRF2014, the JTRF2014 is a time series-based reference frame realized by combining space geodetic inputs including VLBI, SLR, GNSS, and DORIS at a weekly resolution, whose origin is at the quasi-instantaneous CM as measured by SLR. The scale is the weighted average of the quasi-instantaneous scales determined by SLR and VLBI observations. The frame orientation is conventionally aligned to ITRF2008 through the NNR constraint applied to each weekly solution. As a quasi-instantaneous frame, the JTRF2014 attempt to provide stations positions refer to quasi-instantaneous geocenter position. However, the quasi-instantaneous frame was affected by suboptimal network geometry and technique-specific errors along time inevitably. Thus, subsecular variations of geophysical processes and technique-specific errors will represent in the time series of realized quasi-instantaneous frame. Without exception, station position time series indicate inconsistent trajectory with IGS, such as ALGO with not only a constant offset but also unequal amplitude of periodic signals between the two position time series. Stable offsets between the two frame transformation parameters time series indicate long-term mean bias of origin between them. Periodic signals determined

by quasi-instantaneous reference frames are unequal to IGS time series because part of them are absorbed into geocenter non-linear motion.

Likewise, Helmert transformation is performed between JTRF2014 and the corrected IG2 solutions. JTRF2014 is a quasi-instantaneous frame and unable to access to the period after Feb. 2015, so only IGS solutions from 1995 to 2014 are compared in this section. The corrected transformation parameter time series and their amplitude spectrums are displayed in Fig. 11. The offset and drift results from linear regressions to the transformation parameter time series are provided in Table 2.

Table 2
Offsets at epoch 2010.0 and drifts of the transformation parameter time series estimated between JTRF2014 and IGS

	T_X	T_Y	T_Z	R_X	R_Y	R_Z	Scale
offset	-2.1	-0.6	-1.2	-49.3	-5.2	2.4	0.4
drift	-0.10	0.03	0.21	-5.72	4.25	2.87	0.05
Note: Unit for transformation parameters are the same as Table 1.							

Translation time series with greater mean biases shown in Fig. 11 indicate the deviation degree between the instantaneous origin of JTRF2014 and long term mean origin of IGS14. Linear fits of the translation drifts are statistically zero for Y components. Drifts of -0.10 and 0.33 mm/yr are found for X and Z component in the long-term fitting, respectively. The amplitude spectra are represented in the corresponding right panels of Fig. 11. Unlike former analysis, significant spectrum peaks at the annual, to a less degree, semi-annual frequency, are visible in translation time series, whose nature is geophysical and mostly related to mass transformation of the earth surface, and to a large extent, eventually reflect real seasonal geocentric motion and just a fraction of spurious signals due to technique-dependent errors (Blewitt et al. 2002). In addition, the time-variable trend is in poor agreement with the long-term averages, which imply that the SLR-determined origin is not only nonlinear but also with short-term variation trend. Therefore, using a long-term averaged origin of SLR observations to describe geocenter motions of the solid earth like ITRF2014 and DTRF2014 seems not rigorous.

The rotation offsets between JTRF2014 and the corrected IG2 solutions, together with corresponding amplitude spectra are reported in the 4th to 6th rows of Fig. 11. Although both JTRF2014 and IG2 are uniformly aligned to ITRF2008, time series of rotation parameters reveals linear inconsistency over time. The trends of each component are 5.7, 4.2, 2.8 uas/yr respectively, which imply that the rotational alignment of JTRF2014 and IG2 is consistent at the level of 5.7 uas/yr (about 0.2 mm/yr). Except obvious trends, inter-annual variations are contained in time series of rotations too. Particularly, annual amplitudes estimated for X and Y component are 18.46 and 10.04 uas (0.55 and 0.30 mm), respectively. In addition, an abnormal fluctuation is visible in 2010. Largely part of rotation temporal variations come from the biased NNR condition applied at every weekly solution of JTRF2014 due to CN variations (Dong

et al. 2003; Bloßfeld et al. 2014). The worse agreement between JTRF2014 and IG2 may cause significant pole coordinate differences because of the high correlation between pole motion observations and rotations about the X and Y axis (Abbondanza et al. 2020).

It's hard to find out evident seasonal signals and draconitic frequencies of scale offset time series estimated between JTRF2014 and IGS from last row of Fig. 11. Here, non-linear variation of the selected GNSS network vertical component disappears due to the fact that periodic signals are also characterized in the IGS frame. The scale discrepancy between JTRF2014 and the corrected IG2 is up to 1 ppb (about 7 mm in equator). Temporal instability shown in time series of scale offsets are related to SLR-derived scale, which is affected by the degradation of the SLR ground network over time (Altamimi et al. 2007). Besides, a positive long-term linear varying trend (about 0.05 ppb/yr) can be noticed in scale offset time series. The significant variation trend result from the different scale processing strategies adopted by IGN and JPL in averaging the VLBI/SLR information, which indicates JTRF2014 scale averaged by VLBI/SLR observations is significantly disturbed by poor network geometry of the two systems, range biases of SLR (Appleby et al. 2016) and possible VLBI antenna gravity deformation (Sarti et al. 2009, 2010; Gipson 2018). Therefore, the credibility of scale averaged by both SLR and VLBI is still a challenging task when establishing quasi-instantaneous frames. And the urgent requirement for a precise TRF is maintaining and improving the geodetic infrastructure and investigating the causes of technique-specific questions.

Summary And Discussion

The three most recently ITRS realizations, ITRF2014, DTRF2014 and JTRF2014, are regard as most accurate realized TRFs so far. In this paper, the continuous IGS position time series from 1995 to 2020 are used as reference to investigate the characteristics of the three frames by applying Helmert transformation approach. The results from this work are listed as follows:

1. Beyond the data-span of the two secular frames, mis-modeling of equipment changes and earthquakes causing displacement of sites etc. give incorrect positions of sites, while IGS solutions provide continuous and homogeneous positions.
2. PSD models used in ITRF2014 perform better than piece-wise linear model used in DTRF2014 for those sites affected by major earthquakes especially beyond the data-span of the themselves. In addition, short time series of positions used to fit PSD models may generate increasing biases beyond the data-span of ITRF2014.
3. The aligned IGS solutions may also be affected by the mis-modeling of IGb08/IGS14.
4. The translations between ITRF2014 and the IGS solutions demonstrate that good-consistency of origin smaller than 1 mm. The discrepancy of origin between the IGS solutions and DTRF2014 is less than 5.5 mm. Unlike the former two comparisons, the translation offsets estimated between JTRF2014 and corrected IG2 solutions demonstrate inter-annual variations mostly related to the sub-secular variation of the geocenter motion. The time-variable offset existing between JTRF2014 and IGS indicates that using a secular origin to describe the geocenter motion maybe inappropriate.

5. All the three rotation offsets present linear characteristics except the abnormal fluctuations over time. The results prove that the rotation alignment of ITRF2014 and the corrected IGS solutions is of excellent agreement, while the rotation alignment of JTRF2014 and the IGS solutions is at the level of 5.7 uas/yr (about 0.2 mm/yr).
6. Scale offsets between ITRF2014 and the IGS solutions are dominated by annual term, which is related to aliasing of non-linear variations of the station network. Besides a stable offset, the seasonal characteristics of scale offsets between DTRF2014 and the IGS solutions are much similar with the scale offsets between ITRF2014 and the IGS solutions. However, the seasonal signals disappear in scale offsets between JTRF2014 and the IGS solutions. Large instabilities appear in scale offsets related to the quasi-instantaneous scales averaged by VLBI and SLR, which shows uncertainty of the scale up to several millimeters (about 1 ppb). Further investigation is needed to reduce technique-specific errors and set up credible scale processing strategies when establishing neither secular frame nor quasi-instantaneous frame.

According to above analysis, the pivotal conclusions are summarized as follows:

1. Comparing to the two secular frames, IGS frame is more stable than both of them especially for the data-span after 2015. However, the origin and scale of IGS solutions are highly relied on priori frames so that its origin and scale will become inconsistent when a new ITRF is released. Furthermore, the difference between IGS14 and IGS08 may at the level of less than 1 mm due to the antenna calibration updates of specific stations selected in this paper and misalignment of the IGS solutions.
2. The differences between ITRF2014 and DTRF2014 mainly present a linear characteristic. What's more, PSD models used for sites affected by major earthquakes are more preferable especially beyond the data-span of themselves.
3. Quasi-instantaneous frames like JTRF2014 can provide superior reference origin than secular frames whose origin follows the average CM. However, the orientation of JTRF2014 is subject to the biased NNR condition applied at each weekly solution due to CN variations. And JTRF2014 determined scale suffer from large instabilities, which is related to degradation of SLR network over time and technique-specific errors, such as range biases of SLR and mismodel of VLBI antenna gravity deformation et al.

List Of Abbreviations

AC, Analysis Center

CM, Center of Mass

CN, center of network

DORIS, Doppler Orbitography and Radiopositioning integrated by Satellite

GNSS, Global Navigation Satellite System

IGS, International GNSS Service

ITRS, International Terrestrial Reference System

NNR, no-net-rotation

NNT, no-net-translation

NTL, non-tidal loading

PCO, antenna phase center offset

PSD, postseismic deformation

SLR, Satellite Lasor Ranging

TRF, Terrestrial Reference Frame

VLBI, Very Long Baseline Interferometry

Declarations

Ethics approval and consent to participate

Not applicable.

Consent for publication

Not applicable.

Availability of data and materials

The coordinate products from IGS are available at FTP site: ftp://igs.ign.fr/pub/igs/products/$WEEK/repro 2/ and ftp://igs.ign.fr/pub/igs/products/$WEEK/. ITRF2014 solutions and PSD models can be downloaded in ftp://itrf.ensg.ign.fr/pub/itrf/itrf2014/. DTRF2014 solutions can be downloaded in https://doi.pangaea.de/10.1594/PANGAEA.864046?format=html#download. Station position time series are available upon request (richard.s.gross@jpl.nasa.gov).

Competing interests

The authors declare that they have no competing interests.

Funding

This research is supported by the National Natural Science Foundation of China (No.11673050), together with the Key Program of Special Development funds of Zhangjiang National Innovation Demonstration Zone (Grant No. ZJ2018-ZD-009), Key R&D Program of Guangdong province (No. 2018B030325001), and the National Key R&D Program of China (No.2018YFB0504300).

Authors' contributions

JC came up with the idea of the study. JL carried out the experiments and drafted the manuscript. PL write the initial batch script to execute Helmert. WT, DD, and WQ give some comments and suggestions. JC also corrected the manuscript to be more appropriate.

Acknowledgements

We appreciate the International GNSS Service (IGS) for providing the IGS daily solutions. We also thanks to IGN and DGFI-TUM providing ITRF2014 and DTRF2014 frame solutions. Especial thank goes to Richard S. Gross for sending us the station position time series of JTRF2014, so that we can complete the JTRF2014 related parts in the paper.

References

1. Abbondanza C, Chin TM, Gross RS, Heflin MB, Parker J, Soja BS et al (2017) JTRF2014, the JPL Kalman filter, and smoother realization of the International Terrestrial Reference System. J. Geophys. Res. Solid Earth 122:8474-8510. doi:10.1002/2017JB014360.
2. Abbondanza C, Chin TM, Gross RS, Heflin MB, Parker JW, Soja BS et al (2020): JTRF2014: Analysis, Results and Comparisons to ITRF2014 and DTRF2014. In: Z. Altamimi and W. R. Dick (eds.). IERS Technical Note No. 40, Frankfurt am Main: Verlag des Bundesamts für Kartographie undGeodäsie, ISBN 978-3-86482-137-0, pp 17-69.
3. Altamimi Z, Collilieux X, Boucher C (2008) Accuracy Assessment of the ITRF Datum Definition. In: Xu P, Liu J, Dermanis A (eds) VI Hotine-Marussi Symposium on Theoretical and Computational Geodesy. International Association of Geodesy Symposia, vol 132. Springer, Berlin, Heidelberg. https://doi.org/10.1007/978-3-540-74584-6_16
4. Altamimi Z, Collilieux X, Legrand J, Garayt B, Boucher C (2007) ITRF2005: A New Release of the International Terrestrial Reference Frame based on time series of station positions and Earth Orientation Parameters. J. Geophys. Res. 112(B09401). doi:10.1029/2007JB004949
5. Altamimi Z, Collilieux X, Métivier L (2011) ITRF2008: an improved solution of the international terrestrial reference frame. J Geod 85(8): 457-473. Doi: 10.1007/s00190-011-0444-4
6. Altamimi Z, Metivier L, Collilieux X (2012) ITRF2008 plate motion model. J. Geophys. Res. 117(B07402). doi:10.1029/2011JB008930.
7. Altamimi Z, Rebischung P, Collilieux X, Métivier L, Chanard K (2019) Review of Reference Frame Representations for a Deformable Earth. In: International Association of Geodesy Symposia.

Springer, Berlin, Heidelberg.

8. Altamimi Z, Rebischung P, Metivier L, Collilieux X (2016) ITRF2014: A new release of the International Terrestrial Reference Frame modeling nonlinear station motions. J. Geophys. Res. Solid Earth 121:6109-6131. doi:10.1002/2016JB013098.
9. Angermann D, Bloßfeld M, Seitz M, Rudenko S (2020) Comparison of latest ITRS realizations: ITRF2014, DTRF2014 and JTRF2014. In: Altamimi Z and Dick WR (eds.). IERS Technical Note No. 40, Frankfurt am Main: Verlag des Bundesamts für Kartographie undGeodäsie, ISBN 978-3-86482-137-0, pp 79-93.
10. Appleby G, Rodriguez J, Altamimi Z (2016) Assessment of the accuracy of global geodetic satellite laser ranging observations and estimated impact on ITRF scale: Estimation of systematic errors in LAGEOS observations 1993-2014. J. Geod. 1-18, doi:10.1007/s00190-016-0929-2.
11. Argus DF (1996) Postglacial rebound from VLBI geodesy: On establishing vertical reference. Geophys. Res. Lett. 23(9):973-976. doi:10.1029/96GL00735.
12. Argus DF, Heflin MB (1995) Plate motion and crustal deformation estimated with geodetic data from the Global Positioning System. Geophys. Res. Lett. 22(15):1973-1976. doi:10.1029/95GL02006.
13. Argus DF, Peltier WR, Drummond R, Moore AW (2014) The Antarctica component of postglacial rebound model ICE-6G_C (VM5a) based on GPS positioning, exposure age dating of ice thicknesses, and relative sea level histories. Geophys J. Int., 198(1):537-563. doi:10.1093/gji/ggu140.
14. Argus DF, Peltier WR, Watkins MM (1999) Glacial isostatic adjustment observed using very long baseline interferometry and satellite laser ranging geodesy. J. Geophys. Res. 104(B12):29,077-29,093. doi:10.1029/1999JB000237.
15. Blewitt G, Altamimi Z, Davis J, Gross R, Kuo CY, Lemoine FG et al (2010) Geodetic Observations and Global Reference Frame Contributions to Understanding Sea-Level Rise and Variability. In: Understanding Sea-Level Rise and Variability (eds Church J A, Woodworth PL, Aarup T and Wilson WS), Wiley-Blackwell, Oxford, U. K, pp 256-284. doi:10.1002/9781444323276.ch9
16. Blewitt G, and Lavalée D (2002) Effect of annual signals on geodetic velocity. J. Geophys. Res. 107(B7):2145. doi:10.1029/2001JB000570.
17. Bloßfeld M, Angermann D, Seitz M (2018) DGFI-TUM Analysis and Scale Investigations of the Latest Terrestrial Reference Frame Realizations. In: Freymueller J., Sánchez L. (eds) International Symposium on Advancing Geodesy in a Changing World. International Association of Geodesy Symposia, vol 149. https://doi.org/10.1007/1345_2018_47
18. Bloßfeld M, Seitz M, Angermann D (2014) Non-linear station motions in epoch and multi-year reference frames. Journal of Geodesy 88(1):45-63.
19. Borsa AA, Agnew DC, Cayan DR (2014) Ongoing drought-induced uplift in the western United States. Science 345:1587-1590. doi:10.1126/science.1260279.
20. Collilieux X, Altamimi Z, Coulot D, van Dam T, Ray J (2010) Impact of loading effects on determination of the International Terrestrial Reference Frame. Adv Space Res 45:144-154. Doi: 10.1016/j.asr.2009.08.024

21. Collilieux X, and Woppelmann G (2011) Global sea-level rise and its relation to the Terrestrial Reference Frame. J. Geodesy 85(1):9-22. doi:10.1007/s00190-010-0412-4.
22. Danan D, Thomas Y, Heflin M (2003). Origin of International Terrestrial Reference Frame. J. Geophys. Res. 108. 10.1029/2002JB002035.
23. Fritsche M, Sośnica K, Rodríguez-Solano CJ, Steigenberger P, Wang K, Dietrich R et al. (2014) Homogeneous reprocessing of GPS, GLONASS and SLR observations. J Geod 88:625-642. https://doi.org/10.1007/s00190-014-0710-3
24. Fu Y, Argus DF, Landerer FW (2015) GPS as an independent measurement to estimate terrestrial water storage variations in Washington and Oregon. J. Geophys. Res. Solid Earth 120:552-566. doi:10.1002/2014JB011415.
25. Ge M, Gendt G, Dick G, Zhang F P, Reigber C (2005) Impact of GPS satellite antenna offsets on scale changes in global network solutions. Geophys. Res. Lett. 32(L06310). doi:10.1029/2004GL022224.
26. Gipson J (2018) Impact of gravitational deformation in VLBI analysis on the reference frame. In: Abstract G42A-04 presented at AGU fall meeting 2018, Washington, DC, 10-14 Dec
27. Gross R, Beutler G, Plag HP (2009) Integrated scientific and societal user requirements and functional specifications for the GGOS. In: Plag HP, Pearlman M (eds) Global Geodetic Observing System. Springer, Berlin, Heidelberg. https://doi.org/10.1007/978-3-642-02687-4_7.
28. Moreaux G, Capdeville H, Abbondanza C, Bloßfeld M, Lemoine JM, Ferrage P (2020) A comparison of the DTRF2014, ITRF2014, and JTRF2014 solutions using DORIS. In: Z. Altamimi and W. R. Dick (eds.). IERS Technical Note No. 40, Frankfurt am Main: Verlag des Bundesamts für Kartographie undGeodäsie, ISBN 978-3-86482-137-0, pp 95-133.
29. Petit G, and Luzum B (2011) IERS Conventions (2010). IERS Technical Note 36 Verlag des Bundesamts für Kartographie und Geodäsie, Frankfurt am Main, pp 179.
30. Ray J, Altamimi Z, Collilieux X, van Dam T (2008) Anomalous harmonics in the spectra of GPS position estimates. GPS Solutions 12(1):55-64. https://doi.org/10.1007/s10291-007-0067-7
31. Ray JR, Rebischung P, Schmid R (2013) Dependence of IGS Products on the ITRF Datum. In: Altamimi Z, Collilieux X (eds) Reference Frames for Applications in Geosciences. International Association of Geodesy Symposia, vol 138. Springer, Berlin, Heidelberg. https://doi.org/10.1007/978-3-642-32998-2_11
32. Ray JR, Rebischung P, Schmid R (2013b) Dependence of IGS products on the ITRF datum. In: Altamimi Z, Collilieux X (eds) Reference frames for applications in geosciences. IAG Symp, vol 138. Springer, Berlin, pp 63-67. doi:10.1007/978-3-642-32998-2_11
33. Rebischung P, Altamimi Z, Ray J, Garayt B (2016) The IGS contribution to ITRF2014. J. Geodesy 90(7):611-630. doi:10.1007/s00190-016-0897-6.
34. Rebischung P, Altamimi Z, Springer T (2014) A collinearity diagnosis of the GNSS geocenter determination. J Geod 88(1):65-85
35. Rebischung P, Griffiths J, Ray J, Schmid R, Collilieux X, Garayt B (2012) IGS08: the IGS realization of ITRF2008. GPS Solut 16:483-494. https://doi.org/10.1007/s10291-011-0248-2

36. Rebischung P, Schmid R (2016b) IGS14/igs14.atx: a new Framework for the IGS Products. Poster presented at AGU Fall Meeting, San Francisco, CA, Dec. 2016
37. Rietbroek R, Fritsche M, Brunnabend SE, Daras I, Kusche J, Schroer J et al (2012) Global surface mass from a new combination of grace, modelled OBP and reprocessed GPS data. J Geodyn 59-60(5):64-71
38. Rietbroek R, Fritsche M, Dahle C, Brunnabend S, Behnisch M, Kusche J et al (2014) Can GPS-derived surface loading bridge a GRACE mission gap? Surv Geophys 35(6):1267-1283
39. Rudenko S, Bloßfeld M, Muller H, Dettmering D, Angermann D,Seitz M (2018) Evaluation of DTRF2014, ITRF2014, and JTRF2014 by Precise Orbit Determination of SLR Satellites. IEEE Transactions on Geoscience and Remote Sensing 56(6):3148-3158. https://doi.org/10.1109/TGRS.2018.2793358
40. Sarti P, Abbondanza C, Petrov L, Negusini MM (2010) Height bias and scale effect induced by antenna gravity deformations in geodetic VLBI data analysis. J Geod 85(1):1-8. https://doi.org/10.1007/s00190-010-0410-6
41. Sarti P, Abbondanza C, Vittuari L (2009) Gravity-dependent signal path variation in a large VLBI telescope modelled with a combination of surveying methods. J Geod 83(11):1115-1126. https://doi.org/10.1007/s00190-009-0331-4
42. Seitz F (2020) DTRF2014: Information for users. https://www.dgfi.tum.de/en/science-data-products/dtrf2014/information-for-users. Accessed 13 Sep 2020
43. Seitz M, Angermann D, Bloßfeld M, Drewes H, and Gerstl M (2012) The 2008 DGFI realization of the ITRS: DTRF2008. J. Geod. 86:1097-1123.
44. Seitz M, Bloßfeld M, Angermann D, Schmid R, Gerstl M, Seitz F (2016) The new DGFI-TUM realization of the ITRS: DTRF2014 (data). PANGAEA. https://doi.org/10.1594/PANGAEA.864046 (Open Access)
45. Woppelmann G, and Marcos M (2016) Vertical land motion as a key to understanding sea level change and variability. Rev. Geophys. 54:64-92. doi:10.1002/2015RG000502.
46. Wu X, Abbondanza C, Altamimi Z, Chin TM, Collilieux X, Gross RS et al (2015) KALREF—A Kalman filter and time series approach to the International Terrestrial Reference Frame realization. J. Geophys. Res. Solid Earth 120:3775-3802. doi:10.1002/2014JB011622.
47. Wu X, Kusche J, Landerer FW (2017) A new unified approach to determine geocentre motion using space geodetic and GRACE gravity data. Geophys J Int 209(3):1398-1402

Figures

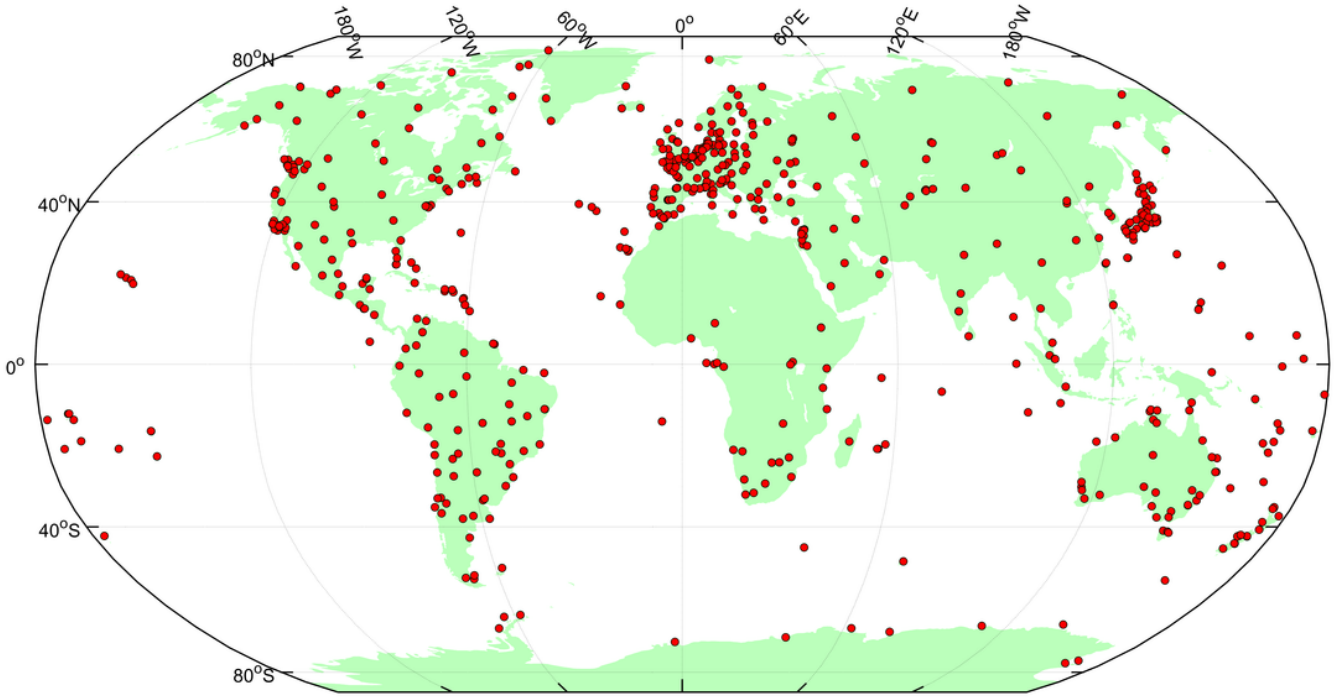

Figure 1

Distribution of IG2 stations. Note: The designations employed and the presentation of the material on this map do not imply the expression of any opinion whatsoever on the part of Research Square concerning the legal status of any country, territory, city or area or of its authorities, or concerning the delimitation of its frontiers or boundaries. This map has been provided by the authors.

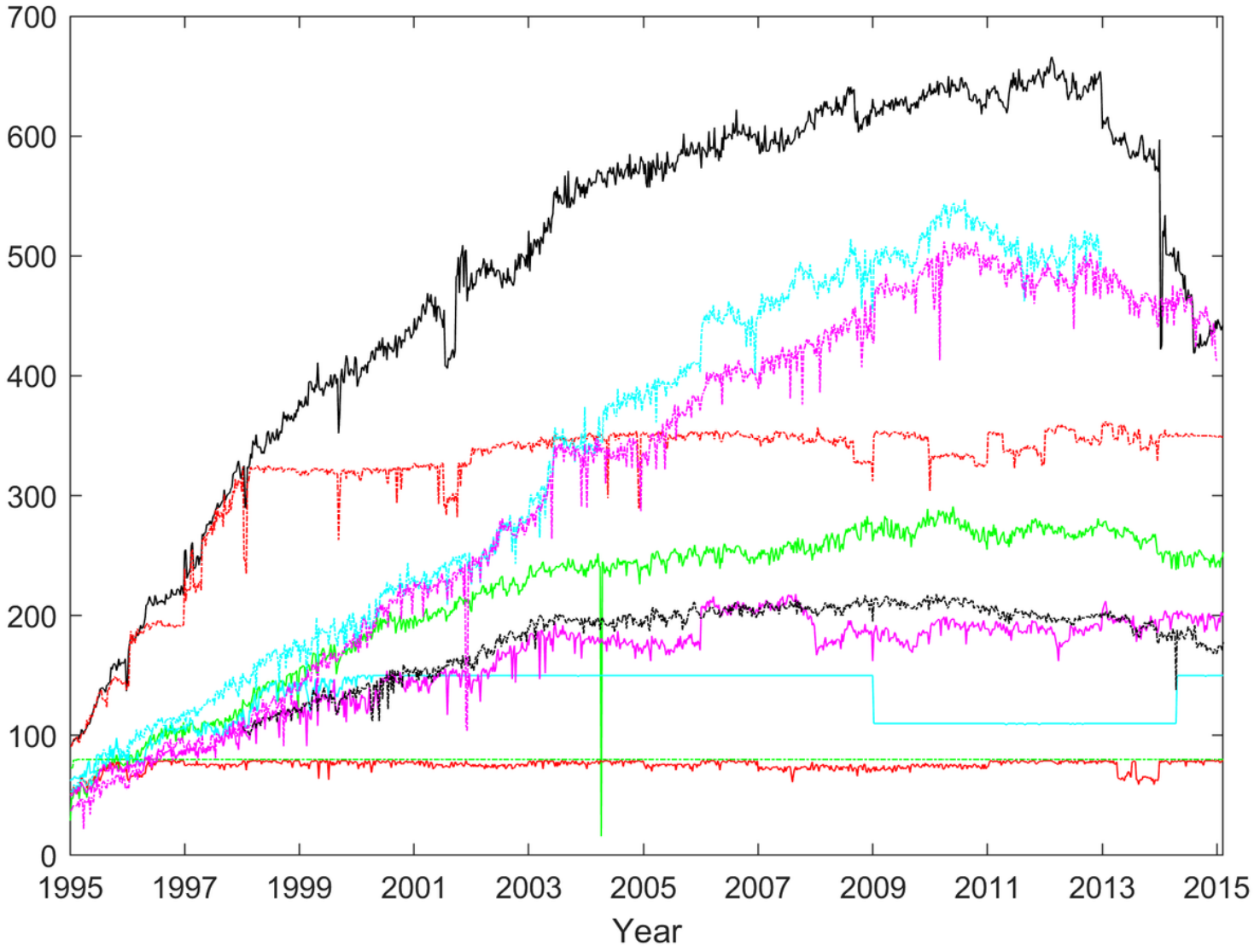

Figure 2

Station number evolution of individual ACs. Black, green, red, cyan and magenta solid lines denote Station number evolution of IG2, COD, EMR, ESA, GFZ respectively, while green, red, cyan and magenta dash dot lines denote Station number evolution of GRG, JPL, MIT, GFZ and ULR respectively.

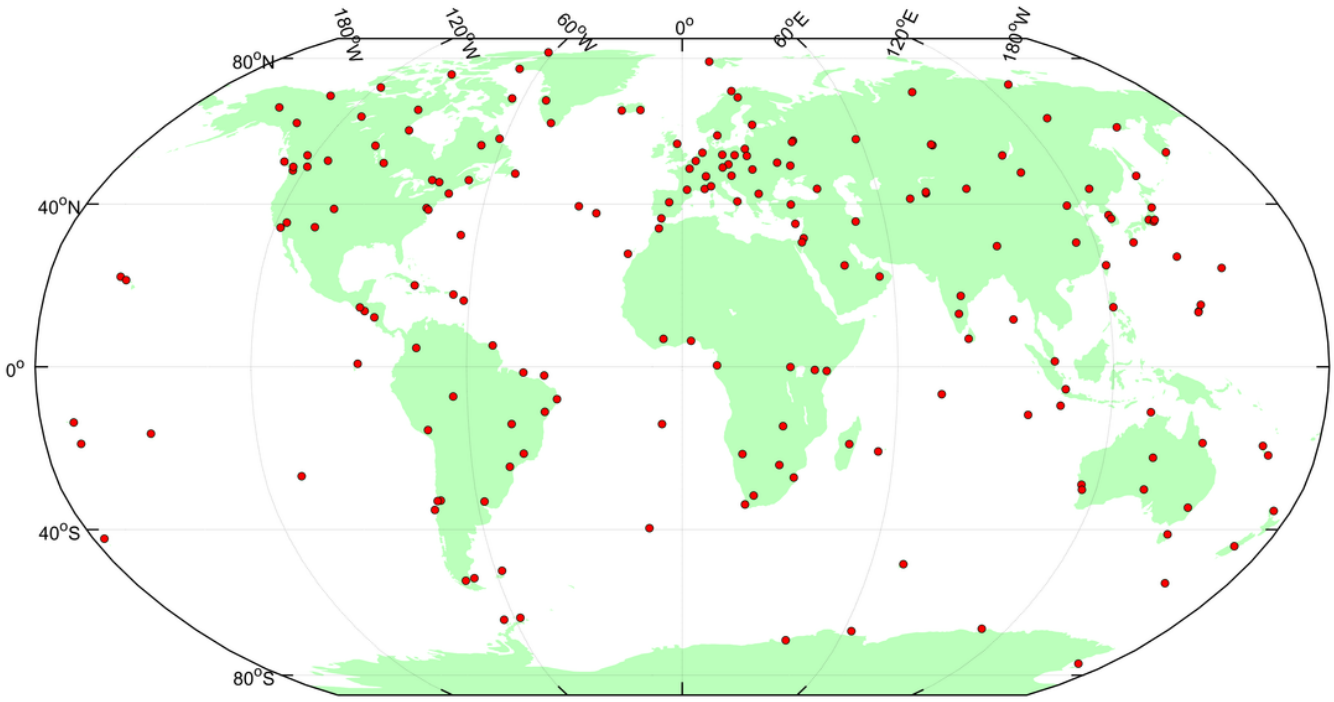

Figure 3

Distribution of the stations involved in Helmert transformation. Note: The designations employed and the presentation of the material on this map do not imply the expression of any opinion whatsoever on the part of Research Square concerning the legal status of any country, territory, city or area or of its authorities, or concerning the delimitation of its frontiers or boundaries. This map has been provided by the authors.

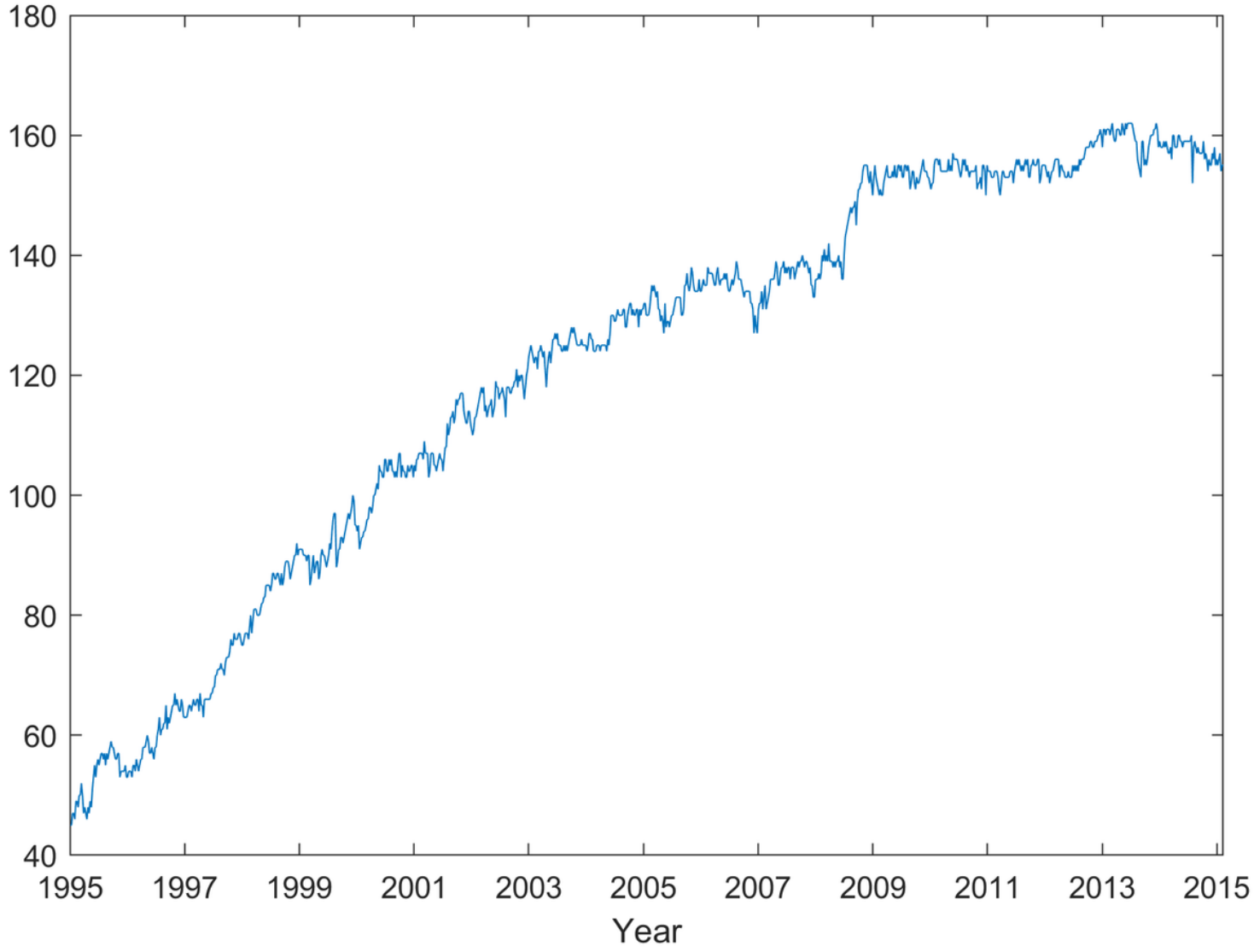

Figure 4

Number evolution of the selected stations

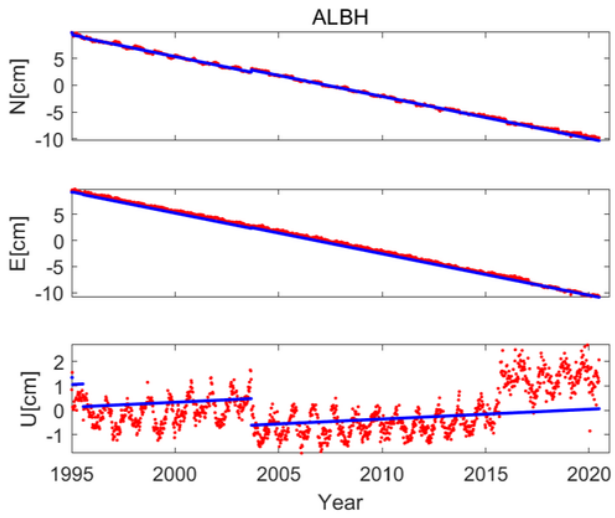

Fig 5a

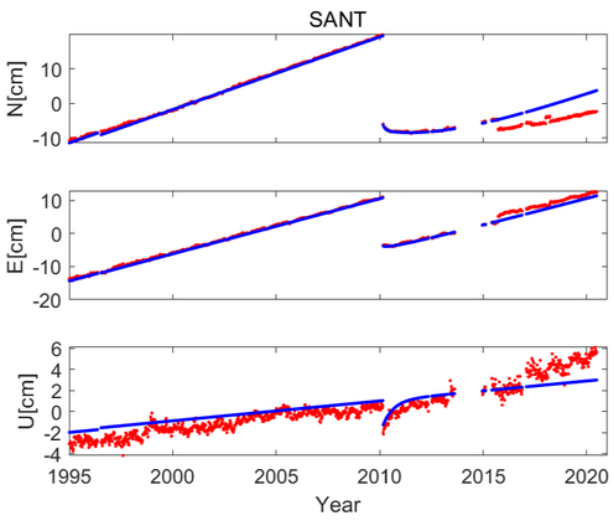

Fig 5b

Figure 5

ITRF2014 and IGS station coordinate time series in NEU coordinate system of ALBH (a) and SANT (b). Note all of them minus average of IGS in individual component. Red and blue dot represent station coordinate time series of IGS and ITRF2014 respectively.

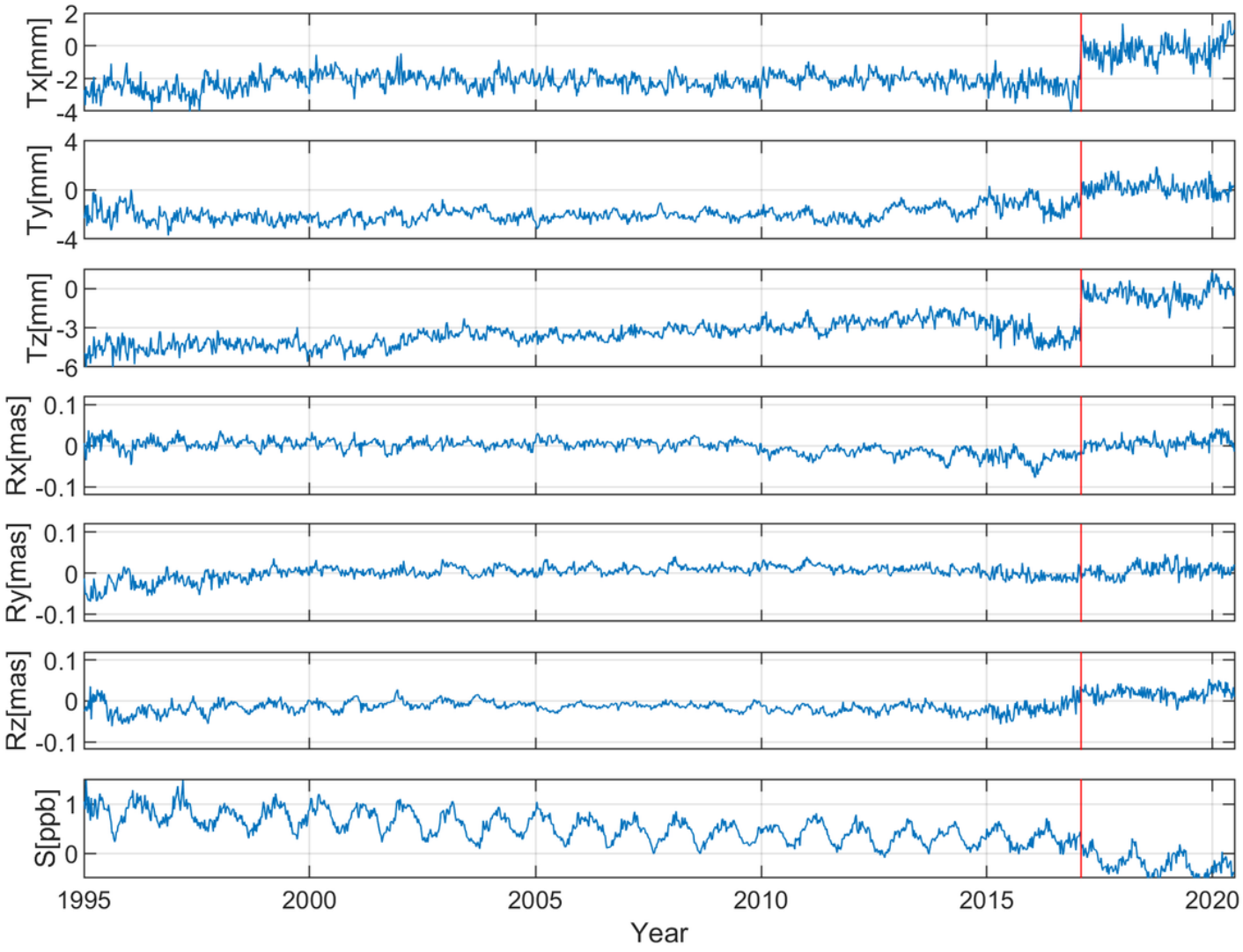

Figure 6

Time series of Helmert transformation parameters estimated between ITRF2014 and IGS. Red vertical lines represent discontinuities occur in IGS time series.

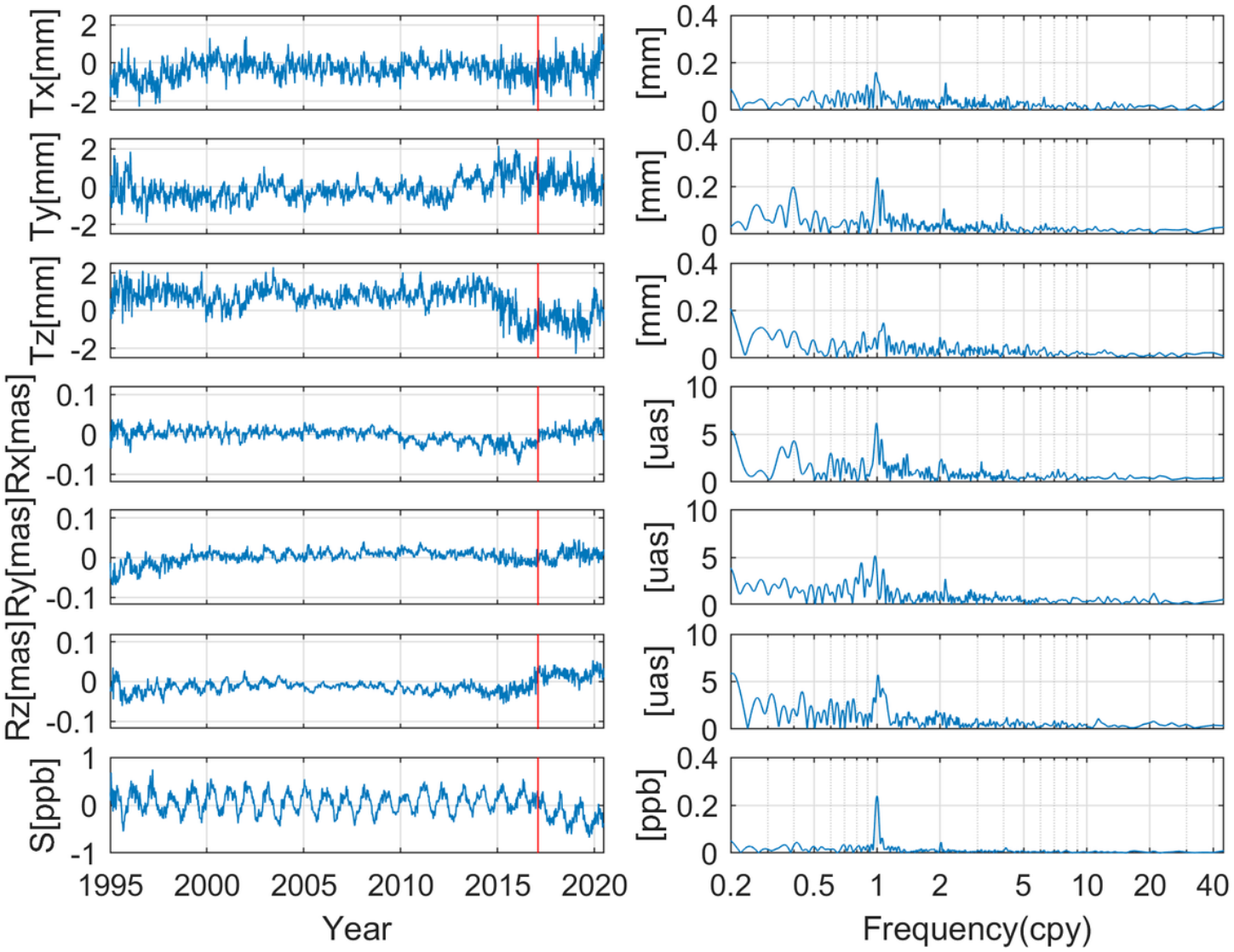

Figure 7

Time series of translation, rotation and scale offsets estimated between ITRF2014 and the corrected IGS solutions and their amplitude spectra from up to bottom; abnormal discrepancies appear in Y and Z components of translation time series from Oct. 2012 to Jan. 2017 may induced by network degradation of IGb08, and prediction mis-modeling of ITRF2014 after Jan. 2017. Scale offsets after Jan. 2017 with an offset about -0.25 ppb/yr are coincident with the long-term scale rate difference of 0.026 ppb/yr and zero-offset at epoch 2010.0 between ITRF2014 and IGS14-based IGS solutions (Rebischung et al. 2016). Red vertical lines represent discontinuities occur in IGS time series.

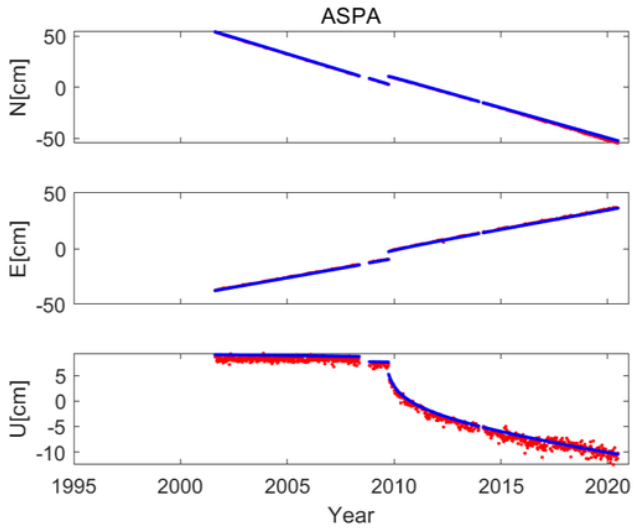

Fig 8a

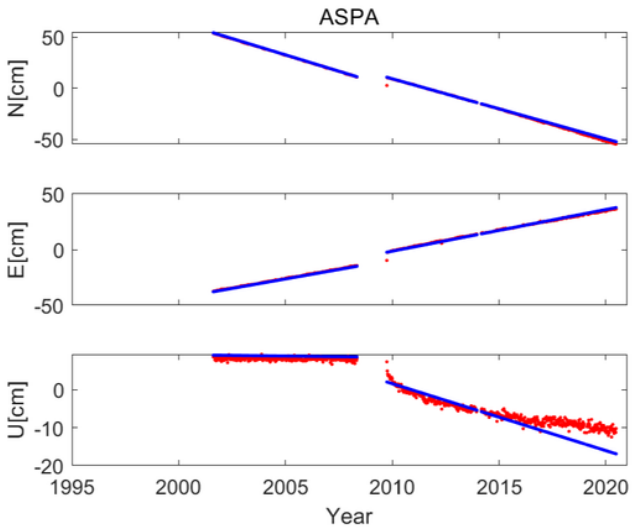

Fig 8b

Figure 8

Station position time series of ASPA. a for ITRF2014, b for DTRF2014, and IGS time series for both a and b as a comparison object. Red and blue dot represent station coordinate time series of IGS and DTRF2014 respectively.

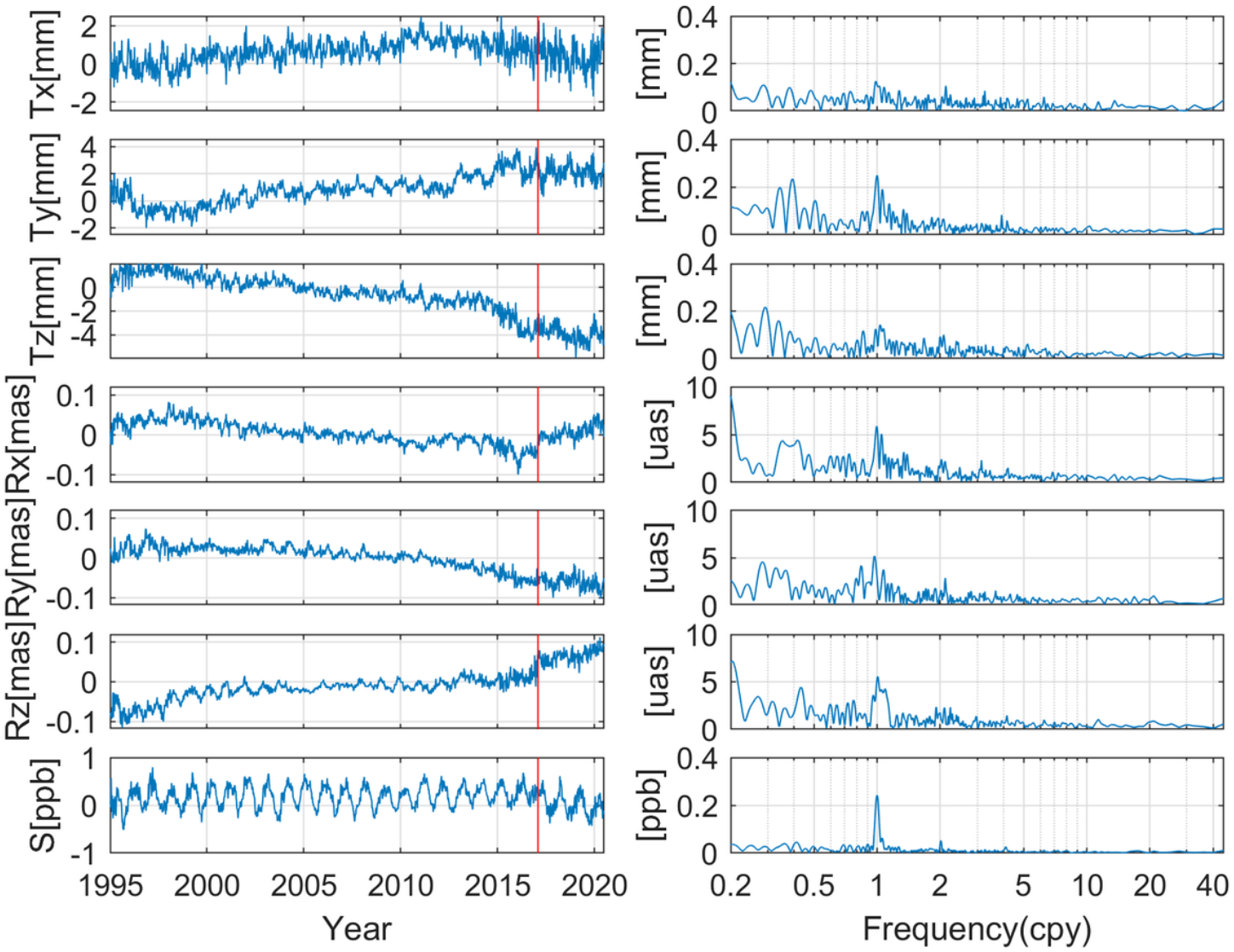

Figure 9

Time series of translation, rotation and scale offsets estimated between DTRF2014 and IG2 and their amplitude spectra from up to bottom. Red vertical lines represent discontinuities occur in IGS time series.

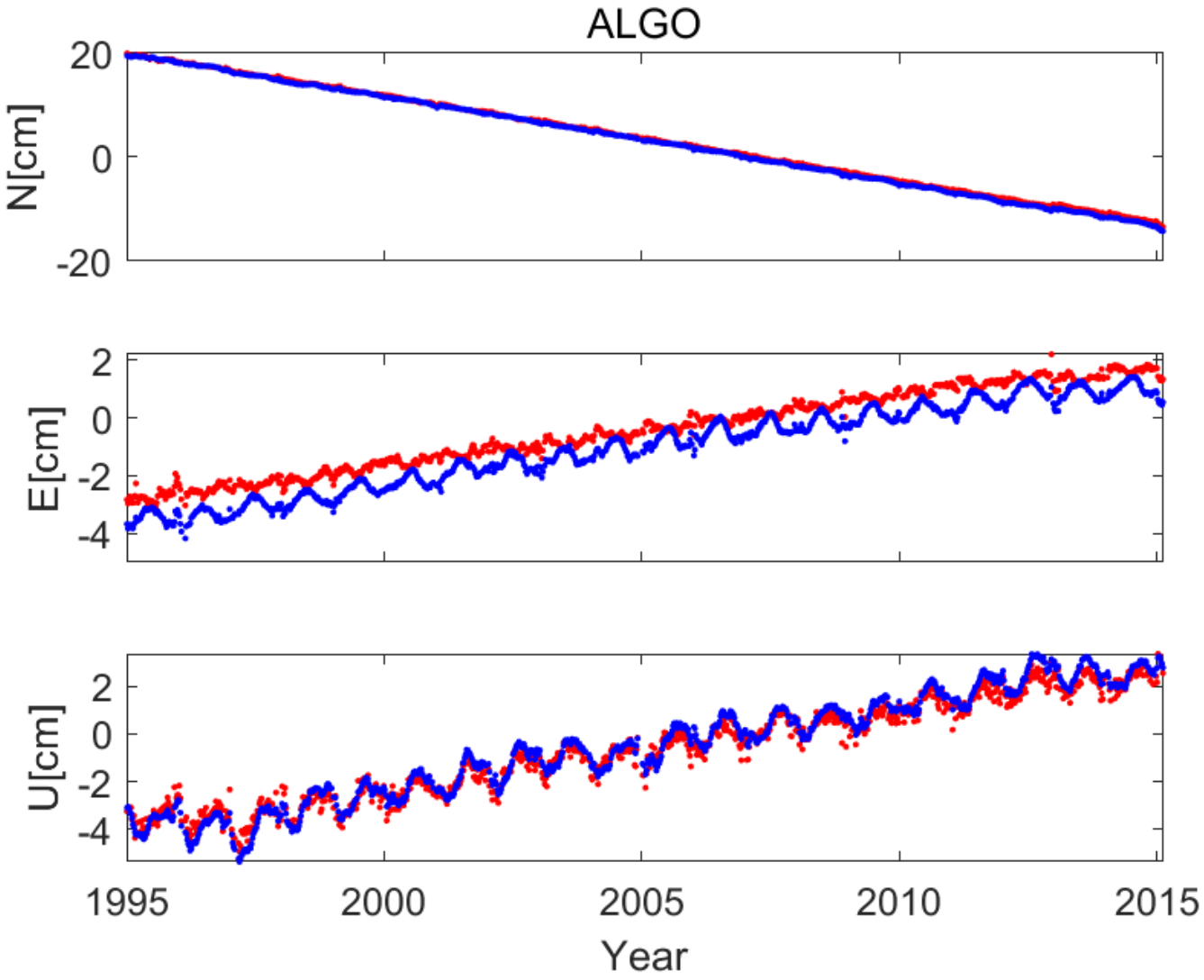

Figure 10

IGS and JTRF2014 station position time series of station ALGO. Red and blue dot represent station coordinate time series of IGS and JTRF2014 respectively.

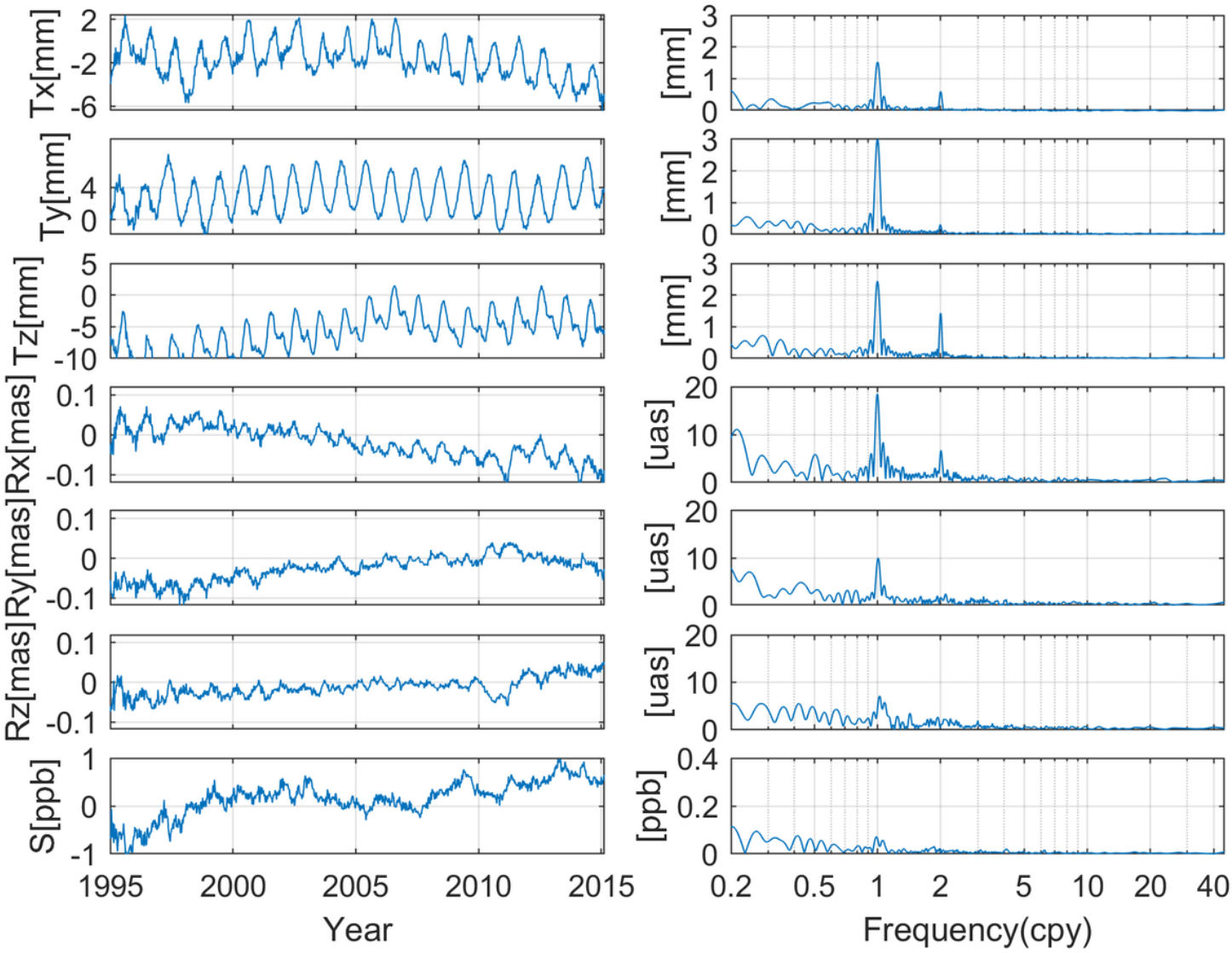

Figure 11

Time series of translation, rotation and scale offsets estimated between JTRF2014 and IG2 and their amplitude spectra from up to bottom

Supplementary Files

This is a list of supplementary files associated with this preprint. Click to download.

- graphicalabstract.png